

dependent propagators ($\beta^{-1}\Omega_j^{-2}$) and with new dipole-moment and potential constants \mathfrak{M}_{1j} , $\mathfrak{B}_3(\lambda\lambda'\lambda'')$, etc., obtained from the original ones M_{1j} , $V_3(\lambda\lambda'\lambda'')$, etc., by unitary transformation with the matrices $U'(\mathbf{k})$. In analogy to Eq. (52), we have

$$\chi^{\alpha\beta}(\mathbf{E}) = \tau^{-1} \sum_j \mathfrak{M}_{1j}^{\alpha} \mathfrak{M}_{1j}^{\beta} / \Omega_j^2. \quad (\text{C8})$$

As previously, some of the apparent field and temperature dependence may be transformed away so that, corresponding to Eq. (54),

$$\chi^{\alpha\beta}(\mathbf{E}) = \tau^{-1} (M_1^{\alpha})^{\dagger} (\omega^2 + C')^{-1} M_1^{\beta}. \quad (\text{C9})$$

As in Eq. (55), the matrix C' is broken up into its diagonal and nondiagonal parts \mathfrak{C} and \bar{C}' , respectively.

$$C' = \mathfrak{C} + \bar{C}', \quad (\text{C10})$$

and expanded as in Eq. (56). In place of Eq. (61), we assume that

$$U' = \exp(i\lambda\mathfrak{B}) = 1 + i\lambda\mathfrak{B} + \mathcal{O}(\lambda^2), \quad (\text{C11})$$

where \mathfrak{B} is of order unity. Equation (67) then follows by substituting Eqs. (C10) and (C11) into Eq. (C5), taking diagonal elements, and using the fact that $[\mathfrak{B}, \omega^2]_{jj} = 0$.

To obtain the matrix element $C'_{jj'}$ between two formerly degenerate soft-mode states j and j' , first solve Eq. (C5) for C' , then substitute Eq. (C11). The result is

$$\begin{aligned} C'_{jj'} &= i\lambda[\Omega^2, \mathfrak{B}]_{jj'} = i\lambda\mathfrak{B}_{jj'}(\Omega_j^2 - \Omega_{j'}^2) \\ &= \mathcal{O}(\lambda)\Omega_j^2 = \mathcal{O}(\lambda)\Omega_{j'}^2. \end{aligned} \quad (\text{C12})$$

We further assume, in analogy to Eq. (58), that for j a nonsoft mode

$$|C'_{jj'}/\omega_j^2| < \lambda \ll 1. \quad (\text{C13})$$

Also, if j' and j are soft and nonsoft modes, respectively, we require that

$$0 < \Omega_{j'}^2/\omega_j^2 < \lambda. \quad (\text{C14})$$

If Eqs. (C12), (C13), (C14), and (67) are substituted into the analog of Eq. (57), Eq. (66) results.

Hybrid Excitons in Diamond*

J. C. PHILLIPS†‡

Bell Telephone Laboratories, Murray Hill, New Jersey

(Received 5 October 1964)

The fundamental reflectivity spectrum of type-IIa diamond has been studied recently by several workers. Our purpose here is to discuss the edge at 7.1 eV which has previously been assigned to the direct threshold $\Gamma_{25'} \rightarrow \Gamma_{15}$. We show instead that a hybrid exciton is present near 7 eV, and that the direct threshold probably occurs at about 8.7 eV. The implications of the revised interpretation for the electronic structure of diamond are also discussed.

1. INTRODUCTION

THE indirect and direct energy gaps in diamond are similar to those in Si. The indirect gap arises from transitions between $\Gamma_{25'}$ and the bottom of the conduction band near X_1 , and occurs at 1.1 and 5.5 eV in Si and C, respectively. The direct gap in Si occurs near 3.5 eV. However, while the line shape neglecting exciton effects is predicted to resemble a step function, the experimental room-temperature spectrum exhibits a peak.^{1,2} The peak in Si has been explained tentatively as an exciton³ (see Fig. 1).

The fundamental reflectivity spectrum of diamond

has been measured recently by several workers.^{4,5} In all cases the optical measurements appear reliable, but rather large differences are found in the observed reflectivity. For example, the percentage reflectance at the largest peak near 12.6 eV is found to be 62%,⁴ or 52%,⁶ or 42%.⁵ Large *qualitative* differences in line shape are found near the 7-eV "direct edge." We believe that at least some of these differences are a result of varying degrees of roughness at the surface of each sample,⁵ and that these conditions drastically alter the lifetimes of exciton resonances. In particular, we

* Supported in part by the National Science Foundation and the National Aeronautics and Space Administration.

† A. P. Sloan Fellow.

‡ Permanent address: Department of Physics, University of Chicago, Chicago, Illinois.

¹ See the experimental data of H. R. Philipp quoted in Ref. 2.

² D. Brust, Phys. Rev. **134**, A1337 (1964); also D. Brust, Marvin L. Cohen, and J. C. Phillips, Phys. Rev. Letters **9**, 389 (1962).

³ J. C. Phillips, Phys. Rev. Letters **10**, 329 (1963).

⁴ H. R. Philipp and E. A. Taft, Phys. Rev. **127**, 159 (1962).

⁵ C. D. Clark, P. J. Dean, and P. V. Harris, Proc. Roy. Soc. (London) **A277**, 312 (1964); P. J. Dean (private communication).

Dr. Dean reports that the best data shown in Fig. 2 used a natural surface. The best polished surface "was examined by multiple-beam interferometry. The surface was found to be very flat, but polishing marks about 10–20- μ wide and 150- \AA deep were detected. Small percussion marks were also revealed under $\times 1200$ magnification which were in small clusters across the surface of the specimen. Freshly cleaved samples showed steps visible to the naked eye."

⁶ W. C. Walker and J. Osantowski, Phys. Rev. **134**, A153 (1964).

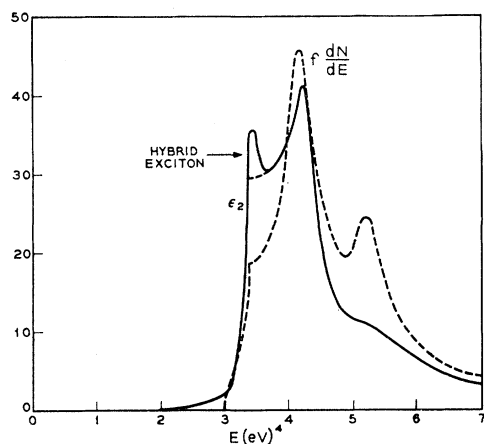


FIG. 1. Spectral dependence of ϵ_2 in Si. Solid line: experimental values at room temperature derived from Kramers-Kronig transform of reflectivity (H. R. Philipp, private communication). Dashed line: theoretical curve based on pseudopotential band model. The experimental peak near 3.4 eV is interpreted as a hybrid exciton. The true interband edges, which were originally believed to be at 3.4 eV, are more probably at 3.7 or 3.8 eV.

show that the structure near 7 eV can be ascribed to a giant exciton resonance with a width $\gtrsim 1$ eV. The situation parallels that in Si, but in diamond, because low-temperature data are available, the evidence is much more complete and convincing.

II. LINE SHAPE NEAR 7 eV

We discuss the line shape of ϵ_2 , the imaginary part of the dielectric constant, near 7 eV. The data we discuss are the reflectance in this region; near the first edge the two are similar, except that as $\omega \rightarrow 0$ one has $\epsilon_2 \rightarrow 0$ and $R \rightarrow 0.2$. Plotting $R(\omega) - R(0)$, we have approximately $\epsilon_2(\omega)$ in the region of interest.^{7,8}

Consider the extreme cases obtained experimentally, the data which show the least structure⁴ and those that show the most.⁵ (The room-temperature data of Ref. 6 agree with those of Ref. 5 at room temperature.) These are shown in Fig. 2. The differences are striking, both as regards different samples at room temperature and the same sample at 295 and 133°K.

To understand these differences, consider the interband spectrum:

- in the one-electron approximation with a static lattice (no excitons, no phonon broadening);
- in the one-electron approximation, with broadening caused by phonon emission;
- including both phonons and excitons.

⁷ The reader may wonder why we have not taken the Kramers-Kronig transform of $R(\omega)$ to obtain $\epsilon_2(\omega)$. The reason is that according to Ref. 6 one obtains *negative* values of $\epsilon_2(\omega)$ near 7 eV when the reflectivity beyond 27 eV is matched to an E^{-4} power law. According to Ref. 8, this difficulty is often encountered in taking Kramers-Kronig transforms. It can be overcome by matching above the experimental cutoff to $E^{-\alpha}$ and adjusting α so that (in our case) $\epsilon_2(5.5 \text{ eV}) = 0$. For our purposes this procedure is almost equivalent to defining $\epsilon_2(\omega) \propto R(\omega) - R(0)$ in the low-energy range.

⁸ M. Cardona (private communication).

First note that the Debye temperature of diamond is 2200°K.⁹ We are very nearly at $T=0$ even at 300°K. The temperature dependence observed in Fig. 2 is therefore quite surprising; we will show that it can be understood in terms of strong, broad excitons.

(a) The one-electron interband spectral density is probably similar in the neighborhood of Γ to that found² in Si; it is illustrated in Fig. 3(a). Because of the threefold degeneracies of $\Gamma_{25'}$ and Γ_{15} the direct threshold (Van Hove edge type M_0) does not occur just at Γ , but occurs about 10% of ΓK away in the $\Gamma K X$ plane. [See Brust's Fig. 10(b)]. The threshold energy is 0.1 eV (in Si; perhaps 0.2 eV in diamond) below that of $\Gamma_{25'} \rightarrow \Gamma_{15}$, which is associated with an M_1 saddle-point edge. The edge is very strong: the absorption may be 100 times stronger than that caused by indirect transitions from $\Gamma_{25'}$ to the neighborhood of X_1 . Because the M_0 and M_1 edges are so closely spaced in energy, near threshold $\epsilon_2(\omega)$ resembles a step function.

(b) We now consider the broadening of the "step function" caused by phonon emission. The direct threshold of GaP appears to have much the same one-electron character as that of Si at and below the edge.¹⁰ Allowing for broadening gives the line shape of Fig. 3(b).

(c) If we compare Fig. 3(b) with the earlier data of Philipp and Taft⁴ good qualitative agreement is found. For this reason their assignment of the edge near 7.1 eV to $\Gamma_{25'} \rightarrow \Gamma_{15}$ was eminently plausible. However, the data of Clark *et al.*⁵ require a different interpretation. The peak, which is strongly temperature-dependent, immediately suggests an exciton. The ex-

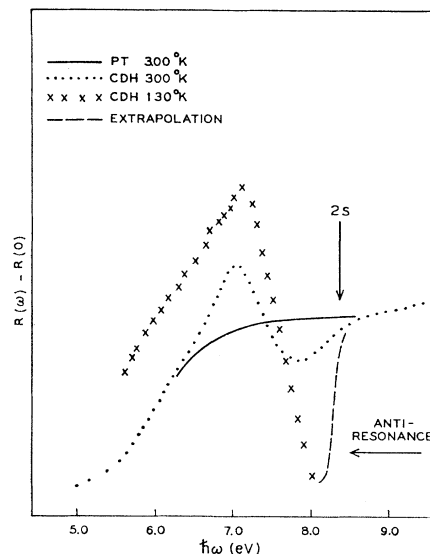


FIG. 2. Experimental values of the reflectivity of type-IIA diamonds near 7 eV according to several sets of measurements. Note the resonance-antiresonance structure which is very pronounced at 130°K.

⁹ J. C. Phillips, Phys. Rev. **113**, 147 (1959); J. L. Yarnell, J. L. Warren, and R. G. Wenzel, Phys. Rev. Letters **13**, 13 (1964).

¹⁰ R. Zallen and W. Paul, Phys. Rev. **134**, A1628 (1964), especially Fig. 6.

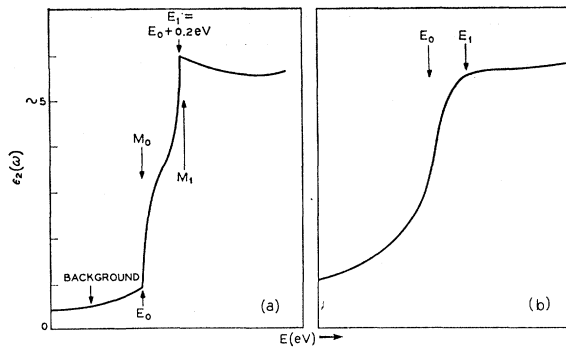


FIG. 3. (a) Direct interband spectrum near threshold in diamond and Si. Because of the quasidegeneracy of the M_0 and M_1 edges the spectral edge resembles a step function. (b) Effect of indirect (phonon-assisted) transitions on the interband spectrum.

citon is very different from that usually found near the direct threshold in semiconductors, because the binding energy is of order 1 eV, and the oscillator strength is very large. For this reason, as well as a more mathematical one discussed below, we refer to the peak as a hybrid exciton.

The strength of the peak can be explained by two circumstances. Compared to other semiconductors diamond has a small static dielectric constant ($\epsilon_0 = 5.5$) which is close to the values found in alkali halides (in KCl $\epsilon_0 = 4.8$ while in NaCl $\epsilon_0 = 5.9$). In the latter typical exciton binding energies are of order 0.3 eV.

In discussing the alkali halides, we have shown¹¹ that two kinds of excitons are present. These are the conventional hydrogenic excitons associated with parabolic interband energy surfaces, and saddle-point excitons associated with hyperbolic interband energy surfaces. The exciton we are dealing with here is a hybrid of these two types, because the exciton binding energy ($\gtrsim 1$ eV) is large compared to the spacing (0.2 eV) of the (quasidegenerate) M_0 and M_1 interband edges.

Both parabolic and saddle-point excitons depend for their existence on the sharp rise in ϵ_2 that occurs near either an M_0 or M_1 interband edge, respectively. When an M_0 and an M_1 edge are quasidegenerate, a very sharp rise resembling a step function is found in ϵ_2 . In three dimensions a dipole-allowed M_0 threshold gives ϵ_2 proportional to $(E - E_0)^{1/2}$ but in two dimensions an allowed threshold gives ϵ_2 proportional to a step function.¹² Thus, a hybrid exciton is qualitatively equivalent to a cylindrically symmetric parabolic exciton with one component of the reduced mass, say $\mu_{zz} = \infty$, while the other two components $\mu_{xx} = \mu_{yy} = m_e \sim m$.

In the relative coordinate system $\mathbf{r} = \mathbf{r}_e - \mathbf{r}_h$, the anisotropic parabolic-exciton problem is equivalent to the donor impurity with an anisotropic effective mass.

This problem has been solved for various ratios of the mass anisotropy

$$\gamma = m_l/m_t. \quad (2.1)$$

The binding energy $E(\gamma)$ in the $1s$ state is given in the limit of extreme anisotropy by¹³

$$E(\infty) = 4E(1). \quad (2.2)$$

The factor 4 in (2.2) accounts qualitatively for the difference in binding energy between the hybrid exciton in diamond and parabolic excitons in the alkali halides.

We now turn to a more quantitative discussion of the exciton line shape. The most striking feature of Fig. 2 is the strong temperature dependence of the resonance peak, followed by an antiresonance which is even more strongly temperature dependent. (It is a pity that the low-temperature data stop near 8 eV because a silica window was used for the vacuum seal.⁵ As sketched in Fig. 2, we believe that this is close to the bottom of the antiresonance, which probably increases above 7.8 eV as indicated, to match on smoothly to the room-temperature curve near 8.3 eV.) The temperature dependence indicates that neither the peak nor the antiresonance amplitude is linear in the effective electron-phonon coupling strength g , where

$$g(T) \propto [1 + 2n(\theta/T)] \quad (2.3)$$

$$n(x) = (e^x - 1)^{-1}. \quad (2.4)$$

The mean phonon temperature θ even of the transverse acoustic modes in diamond is at least 1000°K, so that the change in g from room temperature to 100°K is at most 20%.

Amplitudes strongly nonlinear in g suggest the importance of self-trapping. We have previously conjectured that self-trapping may account for the presence or absence of saddle-point excitons in the alkali halides¹¹ and ionic semiconductors.¹⁴ There is evidence that in thermal equilibrium (microwave experiments on optically injected carriers) holes are self-trapped on diatomic molecules in many of the alkali halides.¹⁵ The self-trapping is accompanied by a Jahn-Teller distortion that forms a halide₂⁻ molecule. Jahn-Teller distortions of N donors in diamond have been observed.¹⁶

Of course, the optical transition takes place much too rapidly to produce large Jahn-Teller effects. However, when the hole is strongly coupled to the lattice (as evidenced by Jahn-Teller effects in thermal equilibrium), one can see that bound-exciton formation will be enhanced compared to electrons and holes in scattering states (because the exciton is neutral, as the lattice was before absorbing the photon). In this way one can understand (albeit only qualitatively) the very strong dependence of the exciton amplitude on g ,

¹³ M. A. Lampert, Phys. Rev. **97**, 352 (1955).

¹⁴ J. C. Phillips, Phys. Rev. Letters **12**, 447 (1964).

¹⁵ T. G. Castner and W. Kanzig, J. Phys. Chem. Solids **3**, 178 (1957).

¹⁶ W. V. Smith, P. P. Sorokin, I. L. Gelles, and G. J. Lasher, Phys. Rev. **115**, 1546 (1959).

¹¹ J. C. Phillips, Phys. Rev. **136**, A1705, A1714 (1964); and Phys. Rev. Letters **12**, 142 (1964).

¹² J. C. Phillips, Phys. Rev. **104**, 1263 (1956).

or on roughness in a surface region of depth 200–300 Å.

We also note that the peak exhibits the asymmetry characteristic of an exciton resonance,¹⁴ i.e., very steep on the high-energy side, less steep on the low side. The asymmetry is a result of interference between the resonance and the indirect background, of a kind well known from the Breit-Wigner theory of nuclear scattering resonances. Ideally, one would like to separate the line width into an intrinsic part Γ and an extrinsic part γ induced by phonon emission or defect or surface scattering. The data shown in Fig. 1 do not permit such detailed analysis, however.

The plateau following the antiresonance is often observed in alkali halides. Hopfield has proposed¹⁷ to identify the shoulder of this plateau with the $2s$ exciton; if this is so, then the series limit which is assigned to $\Gamma_{25'} \rightarrow L_{15}$ occurs at about 8.7 eV.

After completion of this manuscript we received a report from H. R. Philipp and E. A. Taft [Phys. Rev. **136**, A1445 (1964)] which contains a very careful discussion of the reflectance of diamond above 15 eV, and the Kramers-Kronig transforms which yield the optical constants at low energies (see also Ref. 7). While we agree with these authors that the condition $\epsilon_2(\omega) \geq 0$ requires careful treatment of the reflectance at high energies, we also believe that their data do not exhibit the hybrid exciton resonance so completely as the data of Ref. 5 and Ref. 6. Room-temperature reflectivity data only might leave the issue in doubt, but the low-temperature reflectivity data of Ref. 5 demonstrate conclusively that the hybrid resonance is an intrinsic property of very pure diamonds which is extremely sensitive to phonons or (by inference) surface roughness. The structure observed near 16.3 eV in Ref. 6 could also be sensitive to defects and may be intrinsic, although it is not observed by Philipp and Taft in their samples. This point certainly deserves further study because of the unexpected geographical sensitivity of peaks 1–3 eV wide.

III. BAND STRUCTURE OF DIAMOND

At this writing three direct interband edges as well as the $\Gamma_{25'} \rightarrow \Delta_1$ indirect edge are known. It is interesting to compare the theoretical values obtained by OPW calculations^{18,19} with the experimental values (see Table I).

¹⁷ J. J. Hopfield (private communication).

¹⁸ F. Herman, Phys. Rev. **93**, 1214 (1953).

¹⁹ L. Kleinman and J. C. Phillips, Phys. Rev. **116**, 880 (1959).

TABLE I. Comparison of theoretical and experimental energy differences in diamond (in eV).

Edge	Expt.	Theory	δE
$\Gamma_{25'} \rightarrow \Delta_1$	5.5	6.7	-1.2
$\Gamma_{25'} \rightarrow \Gamma_{16}$	8.7 ^a	7.4	+1.3
$X_4 \rightarrow X_1$	12.6 ^b	13.7	-1.1
$L_{3'} \rightarrow L_1$	16.3 ^c	13.6	+2.7

^a This paper.

^b Reference 4.

^c Reference 6.

We see that the agreement, while qualitatively satisfactory, is quantitatively disappointing. In this respect one should remember that diamond, where the atomic cores have the configuration $1s^2$, is by far the easiest semiconductor to treat theoretically. In view of the discrepancies indicated in Table I, further attention should be given to the possibility of “first principles” calculations on diamond.

In conclusion, we note with amusement that the structure proposed here with an indirect edge at 5.5 eV and a direct edge at 8.7 eV is extremely close to that originally proposed on the basis of a pseudopotential model for diamond.²⁰ There the edges were supposed to be at 5.5 and 9 eV, respectively. Although great significance should probably not be attached to this coincidence, it is interesting that even for diamond the pseudopotential approach gives results somewhat more accurate than the best “first principles” calculations now available.

It is a pleasure to thank H. R. Philipp for drawing my attention to Ref. 6, and J. C. Hensel for finding Ref. 16. I have benefited from complete and detailed descriptions of the CDH specimens (see Ref. 5) kindly provided by Dr. P. J. Dean.

Note added in proof. The reader should be apprised that the viewpoint presented here is controversial. In view of the delay attendant upon publication of this manuscript it is with considerable satisfaction that the author draws the reader's attention to the strongly temperature-dependent dip in $\Delta R/E$ found in the optical field effect of Si at 3.4 eV by B. O. Seraphin and N. Bottka, Phys. Rev. Letters **15**, 104 (1965). The exciton dip falls between a dip at 3.35 eV associated with the M_0 threshold and a peak at 3.50 eV associated with the M_1 edge, just as predicted by Fig. 3 of this paper. Further discussion is given by J. C. Phillips and B. O. Seraphin, Phys. Rev. Letters **15**, 107 (1965).

²⁰ J. C. Phillips, Phys. Rev. **112**, 685 (1958).